

Mars Global Surveyor: Aerobraking Mission Overview

Daniel T. Lyons,* Joseph G. Beerer,[†] Pasquale Esposito,[‡] and M. Daniel Johnston*
Jet Propulsion Laboratory, California Institute of Technology, Pasadena, California 91109

and

William H. Willcockson[§]
Lockheed Martin Astronautics, Denver, Colorado 80127

The Mars Global Surveyor spacecraft was launched on Nov. 6, 1996, and was captured into a highly elliptical, 45-h orbit around Mars with a 973 m/s propulsive maneuver on Sept. 12, 1997. A four-month aerobraking phase was supposed to remove another 1200 m/s to circularize the orbit. Unfortunately, one of the two solar wings was damaged during deployment just after launch when the deployment damper failed. What has happened so far to achieve the original mission objectives is described, and the plans for the future of the Mars Global Surveyor Spacecraft are discussed.

Introduction: Brief History

IMMEDIATELY after launch, telemetry indicated that one of the two solar wings had failed to latch. Each of the two Mars Global Surveyor spacecraft (S/C) wings comprise two solar panels and a drag flap (as shown in Fig. 1). The preliminary failure model that explained the postlaunch solar panel deployment anomaly was that the damper shaft had sheared off during deployment.¹ The arm that turned the shaft was believed to be wedged between the inner panel and the yoke and was preventing the panel from latching. Figure 2 shows the position of the panel in the stowed and partially deployed positions with the damper arm still attached to the damper, as well as in the initially deployed configuration, with the damper arm pinched between the yoke and the inboard panel. Figure 2 shows that placing the damper arm between the yoke and the panel would put the panel 24.6 deg from the fully latched position. Because the actual angle was only 20.5 deg, the project analysts concluded that the sharp end of the damper arm had penetrated a short distance into the inboard panel when the panel deployment was abruptly terminated when the damper arm contacted the yoke. An extensive analysis was conducted during the cruise to Mars to both understand the failure and to redesign the aerobraking phase that was scheduled to begin immediately following Mars orbit insertion (MOI). The primary outcome of the redesign effort was that the S/C was reconfigured for aerobraking, as shown in Fig. 1, such that the failed wing (on the $-Y$ side of the S/C) was rotated 180 deg using the inner gimbal to put the active side of the panels on the damaged wing into the flow during each drag pass through the atmosphere. The outer gimbal position was also changed to maintain the same aerodynamic configuration with the solar wings swept back by 30 deg. The reconfiguration was necessary so that the aerodynamic torque at the hinge line would push the hinge toward the closed position because the deployment springs were not strong enough to hold the panel in position against the drag-induced torque about the hinge line.

Minor changes to the sequencing software were required to use a powered mode to hold the outer gimbal in position, rather than the unpowered mode that was still used on the undamaged wing, where the gimbal could be positioned next to a hard-stop. The gimbal motor had to be requalified for the higher holding torque required for aero-

braking in the new configuration. The solar cell sides of the $-Y$ panels had to be requalified at a higher temperature to demonstrate that the cells that would now be directly exposed to the aerodynamic flow could withstand the higher temperatures on the leading side of the wing. Because the gimbal was able to supply sufficient torque and because the cells could withstand the higher temperatures, the basic aerobraking trajectory remained targeted to the originally planned 400-km circular, sun-synchronous 2 p.m. mapping orbit.²

The panel positions for maneuvers using the main engine also had to be changed to minimize the moment around the hinge line to prevent the unlatched panel from shifting during these maneuvers. The capture orbit period was retargeted from 48 to 45 h to reduce the average dynamic pressures and aerodynamic heating required during aerobraking. The periapsis altitude target at capture was reduced from 313 to 250 km to minimize the ΔV required at MOI. The reconfiguration worked as planned, and the Mars Global Surveyor was captured into a highly elliptical orbit around Mars by a 973-m/s main engine maneuver on Sept. 12, 1997. The actual periapsis altitude of 262.9 km was only 12.9 km higher than the 250 km target, whereas the actual 44.993-h orbit period at the first apoapsis was within 25 s of the 45-h target. All of the analyses, testing, requalifications, planning, and software updating had to be completed prior to MOI.

Aerobraking Begins with Redesigned S/C Configuration

Aerobraking began on schedule three orbits after MOI, and proceeded as replanned through orbit 15. The time between the propulsive walk-in maneuvers used to lower the periapsis altitude from the high-altitude capture orbit down to the altitude required for aerobraking was reduced so that the main phase of aerobraking would begin earlier than the original plan. Starting the main phase earlier further reduced the average dynamic pressures and aerodynamic heating.

At MOI, the project analysts believed that the only problem was that the $-Y$ wing was not fully latched. During these early aerobraking orbits, some panel deflection was inferred from the attitude telemetry, but was attributed to elastic deformation near the location where the damper arm was wedged between the yoke and the inner panel of the unlatched wing. Because the panel was not latched, some deflection had been predicted by the structural analyses. There was a moderate uncertainty in the magnitude of the deflection, especially during the early orbits, where the amount of deflection was small. The deflection was inferred from the difference between the expected location of the aerodynamic null attitude and the observed aerodynamic null.³ (The aerodynamic null is the attitude where the aerodynamic moments about the X and Y axes are simultaneously zero.) Other possible contributors to a shift in the aerodynamic null included crosswind, surface accommodation differences between the back of the $+Y$ wing and the cell-side of the $-Y$ wing, flexing or asymmetry in the flaps at the ends of the solar wings, and unmodeled asymmetries in the S/C configuration. As the dynamic

Received Jan. 5, 1998; revision received Aug. 15, 1998; accepted for publication Feb. 22, 1999. Copyright © 1999 by the American Institute of Aeronautics and Astronautics, Inc. The U.S. Government has a royalty-free license to exercise all rights under the copyright claimed herein for Governmental purposes. All other rights are reserved by the copyright owner.

*Senior Engineer, Inner Planets Mission Analysis Group, Navigation and Flight Mechanics Section.

[†]Mission Director, Mars Surveyor Operations Project.

[‡]Navigation Team Chief, Mars Surveyor Operations Project, Navigation and Flight Mechanics Section.

[§]Senior Staff Engineer, Reentry Systems.

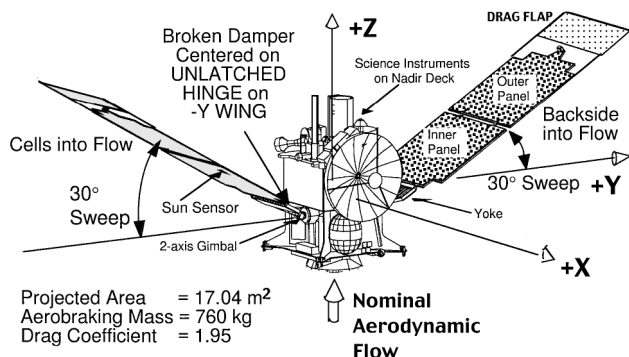


Fig. 1 MGS aerobraking configuration.

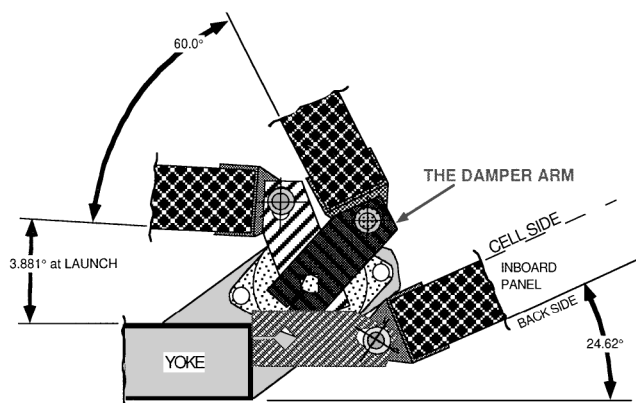


Fig. 2 Detail of the broken solar panel damper assembly.

pressure increased, the apparent offset in the aerodynamic null also increased, as would be expected if one of the panels were connected to the S/C through a spring with a stiffness of about 1100 in.lb/rad.

On orbit 11 accelerometer telemetry near the time of periapsis indicated that the damper arm appeared to shift when the maximum dynamic pressure was pushing on the S/C. Telemetry from a sun sensor mounted on the inner panel of the unlatched wing confirmed that the panel had moved 4 deg closer to the latched position. Near the maximum dynamic pressure on the next orbit, the unlatched solar wing shifted again, this time by 15 deg, such that the panel offset was reduced to nearly zero. The outer gimbal position of the damaged wing was commanded to a new position after each shift to maintain a symmetric aerodynamic configuration with a 30-deg sweep angle to the flow for the next drag pass.

The operations team briefly considered that the panel might have latched into position until the telemetry data from the next orbit indicated that the aerodynamic null perturbation that had been attributed to panel bending was still present. The shifts in the solar panel position implied that the damper arm had moved out from between the yoke and the inner panel such that the hinge had reached the latched position. Because the postulated hinge configuration was such that the wing could not possibly bend about the hinge line beyond the latched position, but the data indicated that the panel was bending beyond the latched position, the failure mode had to be different than the one established during cruise. The project analysts immediately began to examine the telemetry to develop a new failure model that could explain the new data. Possible failure mechanisms were discussed during the next three orbits, while aerobraking continued as planned.

On orbit 15, three orbits after the 20.5-deg kink in the unlatched panel straightened out, the atmospheric density was unusually high (50% larger than on the previous two orbits; see Table 1), and the panel deflection inferred from the dynamic changes in the aerodynamic null implied a huge, 17-deg deflection. Because the magnitude of the deflection on orbit 15 could not possibly be explained by the original failure model, the project manager concluded that the solar wing was not only unlatched, but also damaged more seriously than originally believed. A command was immediately sent

to propulsively raise the periapsis altitude by 11 km to reduce the dynamic pressure from 0.60 to 0.20 N/m² and, thus, reduce the apparent bending to a few degrees. The attitude for the drag pass on orbit 16 was changed so that the sun sensor mounted on the unlatched wing could be used to measure the position of the sun relative to the solar panel during the drag pass and to confirm if the solar wing was bending relative to the inertially propagated S/C attitude. The measured deflection was 3.4 deg, which was close to the value inferred from the shift in the aerodynamic null. On the next orbit (17) a similar technique was used to show that the latched panel did not bend at all, within the 0.5-deg accuracy of the sun sensor measurement. On orbit 18, a second measurement of the deflection of the unlatched panel produced the same 3.4-deg bending at a dynamic pressure of 0.19 N/m². Because the only explanation for the bending was that the solar wing was damaged more seriously than previously thought, the project manager decided to raise the periapsis altitude completely out of the atmosphere until the implications of the damage could be carefully considered. This decision to temporarily stop aerobraking was extremely serious because it meant giving up the ability to reach the 2 p.m. sun-synchronous, 400-km circular mapping orbit for which the spacecraft was designed. It also meant that the remainder of the mission would have to be completely redesigned.

Damage Assessment During the Aerobraking Hiatus

During the 25-day hiatus from aerobraking, a very intensive analysis and ground test program was conducted to determine what failure would explain the panel deflection and what could be done to re-plan the mission. The most likely failure scenario that emerged from this hiatus was that one of the yoke facesheets had cracked when the undamped panel stopped abruptly during deployment (Fig. 2). The yoke is similar in construction to the solar panels, with two graphite epoxy facesheets separated by an aluminum honeycomb. Ground tests and analysis both showed that the most likely failure was a cracked facesheet on the yoke, near the gimbal motor where the yoke is narrowest. The crack was believed to follow a stress concentration where the facesheet thickness was reduced from double to single thickness. Only the facesheet on the compression side (back side; see Fig. 2) was believed to be broken because the graphite epoxy is not as strong under compression and because the yoke used for ground testing broke on the compression side. The other facesheet is believed to be intact and is providing the restoring moment that brings the solar wing back to the undeflected position after each drag pass. Further analysis and ground testing of a broken yoke at various load levels for many cycles resulted in a maximum acceptable dynamic pressure level of 0.6 N/m² for the thousand cycles that were needed to achieve a sun-synchronous, 400-km circular mapping orbit at a reduced dynamic pressure. Of course, there was no way to guarantee that the damage to the flight hardware was the same as the damage to the ground test hardware or that the number of cycles placed on the ground test hardware was representative of the number of bending cycles that the flight hardware could survive.

Before aerobraking was resumed, a set of criteria was selected to enable the project analysts to determine if the panel characteristics of the flight hardware were changing in a way that would indicate a weakening of the yoke stiffness. These characteristics include the bending stiffness, which is inferred from the measured bending angle and the measured maximum dynamic pressure, and the natural frequency of the solar wing, which is measured by S/C attitude and acceleration perturbations using the inertial measurement unit. Both the stiffness and natural frequency will decrease if a crack begins to propagate on the undamaged side of the yoke. The return angle of the wing after each bending event is also monitored using the sun sensor on the unlatched panel and compared to the return angle on previous orbits. These parameters are evaluated after each pass through the atmosphere and contribute to the daily decision process for what is an acceptable level of drag for the coming orbits. The natural frequency attributed to the bending mode of the damaged wing, 0.166 Hz, has been relatively constant ever since launch. The accelerometer data showed that this 0.166-Hz mode is strongly excited on some orbits, as though the cracked edges might

Table 1 Key events during phase 1 of aerobraking

Orbit number	Date	Altitude, km	Period, h	Dynamic pressure, N/m ²	Comments
1	9/12/1997	262.9	45.0	0	MOI
4	9/17/1997	149.3	44.9	0.004	First drag pass, sun crosses equator into southern hemisphere.
8	9/25/1997	116.1	44.0	0.23	AACS anomaly, no telemetry
10	9/28/1997	116.4	42.8	0.23	S/C commanded to contingency mode to reinstate attitude knowledge
11	9/30/1997	111.2	42.2	0.49	0.2 m/s maneuver, panel shifts 4 deg at periapsis
12	10/2/1997	110.5	41.0	0.53	Panel shifts 15 deg at periapsis, is panel latched?
13	10/3/1997	110.3	40.0	0.64	Aeronull still offset, bending? 0.18-Hz vibration still present
15	10/7/1997	110.0	37.5	0.90	Unexpected 50% density spike aeronull offset \Rightarrow 17-deg bending?
16	10/8/1997	121.0	36.5	0.20	Periapsis is raised, $-X$ to nadir for bending measurement of $-Y$, sun sensor measured 3.4-deg bending
17	10/10/1997	120.9	36.2	0.23	$+X$ to nadir, panel flipped for bending measurement of $+Y$, sun sensor measured 0 deg
18	10/11/1997	121.2	35.7	0.19	$-X$ to nadir for bending measurement of $-Y$ (still bending 3.4 deg)
19	10/13/1997	171.7	35.5	0.0005	Begin hiatus, periapsis raised out of atmosphere, science data are collected while analyses, tests, and redesign worked in parallel
37	11/8/1997	134.8	35.2	0.026	Resume aerobraking phase 1 with first walk-in maneuver
41	11/14/1997	124.4	34.8	0.16	Accelerometer data show unusual step followed by panel ringing with 6-s period
50	11/26/1997	123.5	32.0	0.14	Lower than average dynamic pressure, lower periapsis? (It is not.)
51	11/28/1997	123.7	31.7	0.32	133% increase in dynamic pressure signals start of dust storm, pair of raise maneuvers commanded
52	11/29/1997	131.7	31.3	0.06	Density drops back close to what was expected
53	11/30/1997	131.6	31.3	0.15	Density continues to increase, pattern of high and then low densities is correlated to longitude wave 2
70	12/22/1997	125.1	27.8	0.24	Dust storm effects have disappeared
82	1/4/1998	122.3	24.8	0.21	Start of eclipse region
85	1/7/1998	121.1	24.0	0.26	Mars perihelion (aphelion 12/17/1998)
110	1/29/1998	120.5	19.3	0.30	1st MOLA warming slew maneuver
114	2/2/1998	121.2	18.8	0.21	First draft of this paper completed
125	2/10/1998	117.3	17.4	0.22	Maximum eclipse of 58.1 min, 46.8% depth of discharge
132	2/15/1998	117.1	16.6	0.31	Emergency Aerobrake Planning Group to discuss huge difference between peak density and average density, peak dynamic pressure 0.452 N/m ²
141	2/21/1998	116.1	15.7	0.41	Highest dynamic pressure in phase 1 accelerometer peak = 0.483 N/m ²
142	2/21/1998	118.4	15.5	0.21	7.7-deg panel deflection, alarms tripped After periapsis raised by 0.148 m/s maneuver at apoapsis, large solar wing ringing on orbit 143
194	3/23/1998	119.8	11.7	0.16	Begin reducing dynamic pressure to slow rate of period decay to hit orbit period target for SPO
201	3/27/1998	125.1	11.5	0.05	Last aerobraking orbit in phase 1
202	3/27/1998	170.7	11.5	0.0008	First SPO
223	4/6/1998	172.7	11.5	0.0003	Periapsis at north pole, target pole with Mars Orbiter laser altimeter
268	4/28/1998	174.1	11.5	0.0002	Begin conjunction seq, no science
309	5/18/1998	176.1	11.4	0.0002	Last eclipse orbit during SPO
329	5/28/1998	176.8	11.4	0.0002	Resume science after conjunction
433	7/17/1998	176.6	11.4	0.0002	Sun crossed equator northward
573	9/23/1998	171.1	11.5	0.0015	Last SPO
574	9/24/1998	126.9	11.5	0.05	Begin phase 2 walk-in

be suddenly slipping past each other while under compression from the aerodynamic moment. The return angle after each drag pass eventually returns to zero, but an unusual 1-deg bend was observed to build up sometime during the eclipse preceding the drag pass during phase 1 of aerobraking. This bending is believed to be thermally induced. The amount of bending during the drag pass has remained about 4 deg for a typical dynamic pressure of 0.25 N/m² near periapsis.

Mission Redesign During the Hiatus

Because the original plan^{4,5} to achieve a mapping orbit with a 2 p.m. mean local solar time at the descending node required average dynamic pressures equal to the new not-to-exceed value of 0.6 N/m² and because aerobraking had been put on hold for one-fifth of the planned aerobraking duration while the project analysts determined the extent of the damage, the originally planned 2 p.m. mapping orbit could no longer be achieved. After consulting with the Project

Science Group (PSG), the project manager concluded that achieving a circular orbit was essential for meeting the mission objectives. The PSG selected a 2 a.m. mean local solar time sun-synchronous mapping orbit as the new target. The new mapping orbit is essentially the same as the originally planned mapping orbit, except that the sun is near the ascending node rather than the descending node.⁶ (To be consistent, the local solar time is still measured at the descending node.) Because the orbit plane precesses very slowly for orbit periods larger than 4 h, the local solar time (LST) changes as Mars moves around the sun. Therefore, the LST of the mapping orbit is primarily determined by the date near the end of aerobraking, where the orbit period drops below 4 h, and the precession rate approaches a sun-synchronous rate. Thus, the next opportunity for a 2 a.m. orbit was early in February 1999.

Aerobraking Resumed After the Hiatus

Once the project manager decided that it was not only necessary to resume aerobraking to continue the mission, but also reasonably safe, a new plan was developed to reach the new 2 a.m. mapping orbit target. Phase 1 of aerobraking resumed on Nov. 8, 1997, on orbit 37. The plan was to keep the expected dynamic pressure below 0.3 N/m², which maintains a 100% density margin relative to the redesigned dynamic pressure limits. A 100% margin was included in the original plan for random atmospheric density fluctuations.

Before reaching the new 2 a.m. LST target, Mars passed directly behind the sun at conjunction on May 12, 1998. Aerobraking could not be conducted while Mars was in conjunction, and so a propulsive maneuver was necessary to terminate aerobraking in early May. (All of the propulsive maneuvers through the end of phase 1 of aerobraking are described in a paper⁷ by the navigation team.) The new mission plan took advantage of the opportunity afforded by the need to suspend aerobraking for conjunction by establishing a 5-month period after conjunction for unique science observations in an elliptical orbit employing a very low periapsis, dubbed the science phasing orbit (SPO). Low-altitude (high-resolution) imaging, Phobos imaging, targeted surface imaging, and unique electron reflectometer and high resolution magnetometer measurements were made possible by the SPO. The SPO phase began when periapsis was propulsively raised up out of the atmosphere on orbit 201 (March 27, 1998), when the orbit period reached the predetermined value of 11.5 h about a month and a half before the communications blackout at conjunction. Targeting a specific orbit period was important for avoiding a resonance orbit, which could have resulted in large gravitational perturbations to the inclination.

Before conjunction, the Mars Global Surveyor (MGS) S/C collected science data, including targeted observations of high-priority surface features, up to the point where commands could not be reliably sent to the S/C (April 28, 1998), at which point the S/C was put into a safe configuration until reliable communications could be restored after conjunction (May 28, 1998).

As SPO implies, the instruments were turned on and pointed at nadir near periapsis to record science data that were played back later in the orbit when the high-gain antenna was pointed at the Earth. During the pre-conjunction science gathering phase, some very interesting targeted observations of specific surface features were made.⁸ The SPO carried the S/C through conjunction and continued to orbit 573 on Sept. 23, 1998, when phase 2 of aerobraking began. The MGS S/C will continue phase 2 of aerobraking until about orbit 1325 (Feb. 9, 1999), when the periapsis altitude will be raised out of the atmosphere for the final time when the apoapsis altitude reaches 450 km.

Because the attitude control system uses between 5 and 10 g of propellant on each pass through the atmosphere and because the propellant budget is very tight, the project analysts had to minimize the number of aerobraking orbits. Because the 2 a.m. mapping orbit is roughly determined by the date where Mars is on the other side of the sun from the initial target date for the start of mapping, delaying the start of phase 2 reduced the number of aerobraking orbits (and, thus, reduced the attitude control propellant required for aerobraking).

ing) but increased the average dynamic pressure on each orbit from what it would have been if aerobraking had resumed immediately following conjunction. Even though phase 2 started Sept. 23, 1998, one week later than planned, the average dynamic pressure will be less than the average for the latter part of phase 1, so that there will be margin available in case there are unpredictable delays or greater atmospheric variability during phase 2.

Complications Created by the New Aerobraking Plan

The operations team has faced many challenges due to the unplanned extension of aerobraking. The S/C was designed to operate in a 2-h, sun-synchronous mapping orbit around Mars. The maximum eclipse for the planned nearly circular mapping orbit was only 40 min. Because the S/C is traveling much slower near apoapsis of the highly elliptical aerobraking orbit, the eclipses have the potential of being much longer than 40 min. In fact, the maximum eclipse duration of the first eclipse season in early February of 1997 was 58 min, 45% longer than the maximum design requirement. Surviving the eclipse meant that the solar panels had to survive very cold temperatures that nearly reached the requalification limits, in spite of the intensive effort to reconfigure and operate the S/C to maximize the panel temperatures at the entry into eclipse.

Another challenge associated with the longer than planned eclipse duration was the depth of discharge on the batteries. The batteries reached a maximum depth of discharge of 48%, which meant that the S/C would survive one battery failure, but the lifetime of the remaining battery would have been significantly reduced if one of the batteries had failed. Both batteries were still fully functional following the first eclipse season. The larger than desired depth of discharge means that the expected battery life has been slightly reduced, but not enough to jeopardize the planned 2-year (1 Mars year) mapping mission, which will put many cycles on the batteries when there is an eclipse every orbit. As long as aerobraking continues on schedule, the next maximum eclipse will be less than the 40 min that is typical for the mapping orbit. If the S/C does not reach an orbit period of about 6 h before the next eclipse season, which begins near the end of phase 2 of aerobraking, the maximum eclipse will be larger than 60 min, which would severely stress the S/C hardware. Thus, it is very important that aerobraking proceed as replanned.

Another operations complication due to the longer aerobraking phase is that the instruments could get too cold if the original aerobraking sequence were used. The instruments are located on the +Z face of the S/C, whereas the undeployed high-gain antenna is mounted 90 deg away, on the +X face, as shown in Fig. 1. During the original aerobraking sequence, the S/C would spend most of the time in array normal spin (ANS), with the +X axis toward the Earth to maintain a high-rate telecommunications link, and a 100-min rotation about +X so that the body-fixed star sensor can detect stars that are used to update the inertial reference. During the originally planned aerobraking phase, there was always some sun available during part of the ANS rotation to warm the instrument deck. Because aerobraking will now take much longer to complete, Mars reached conjunction in the middle of the redesigned aerobraking phase, before the high-gain antenna was deployed. Near conjunction, when the sun and Earth are close together in the sky as viewed from Mars, the +Z face is in the shadow of the high-gain antenna (HGA) on the +X face (see Fig. 1), so that the instruments are not warmed by the sun at anytime during the 100-min spin. The onboard sequence was modified to include two inertial slews to tip the +Z face toward the sun (and the +X axis, HGA boresight away from Earth) to keep the instruments warm.

Maintaining sufficient propulsive maneuver propellant has been another challenging task. The original plan did not have a very large propellant margin to begin with. The periapsis altitude has already been raised out of the atmosphere, and then returned for the hiatus, and then raised out again at the start of the SPO, and returned for the start of phase 2. The ΔV budget contains enough fuel for only one additional periapsis raise/lower in case of an anomaly during aerobraking.

During phase 2 of aerobraking, there is not enough time in the orbit to play back very much recorded science data, so that the project

⁸A link to a discussion of these observations can be found at <http://marsweb.jpl.nasa.gov>.

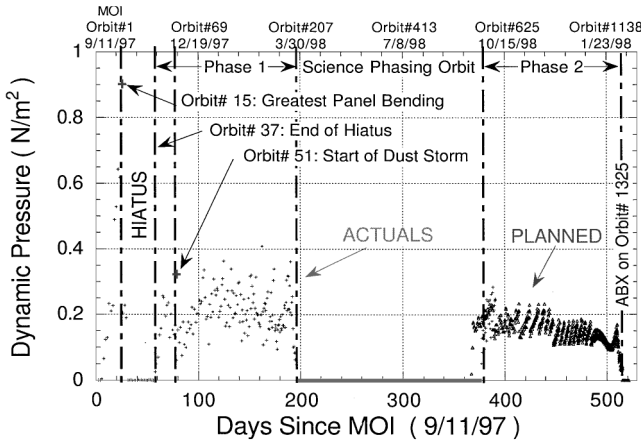


Fig. 3 Dynamic pressures at periapsis: actual and planned.

analysts will have to use other means, such as the accelerometer and the horizon sensor, to detect the mission threatening atmospheric density increases that can accompany a global dust storm. Although phase 2 occurs as Mars approaches aphelion, where global dust storms are believed to be less frequent, dust storms have been observed at every season on Mars and will be a continued threat.

New Aerobraking Trajectory

The aerodynamic pressure at periapsis, $\frac{1}{2}\rho V^2$, is one of the most important aerobraking parameters. If the average dynamic pressure is too low, aerobraking will take too long, and the spacecraft will not reach the desired LST for the mapping orbit. If the dynamic pressure is too high, then the S/C will be damaged. Figure 3 uses + symbols to show the dynamic pressure history (reconstructed by the navigation team) from MOI (MOI is orbit 1) through Oct. 4, 1998 (orbit 600). The events leading up to the hiatus that started on orbit 19 were discussed earlier. The most significant event during the remainder of phase 1 was the dust storm that began around orbit 51.

The primary reason that there is at least 100% margin on the expected dynamic pressure compared to the flight allowable is to accommodate both random variability in the atmosphere and the initially rapid monotonic density increases due to global dust storms near the surface. The periapsis altitude must be raised propulsively to accommodate the order of magnitude density increase that was predicted by prelaunch atmospheric simulations of the initial phase of a global dust storm by atmospheric scientists at the NASA Ames Research Center, the NASA Marshall Space Flight Center, and the University of Arizona. The simulations showed that the maximum density occurs only a few days after the start of a dust storm because the high winds can quickly spread enough dust through the atmosphere to allow significant solar warming and expansion of the middle atmosphere, which increases the densities at a given altitude everywhere above the heated region. Thus, the project plans included an extensive observing campaign to monitor dust levels in the atmosphere of Mars during the aerobraking phase. These observations were particularly critical because aerobraking had to take place during the so-called dust storm season centered on Mars perihelion, where most large dust storms had been observed in the past.

On orbit 51, only 14 orbits after aerobraking resumed following the hiatus, the atmospheric density increased by 133% from the value on the previous orbit. This increase was four times larger than the variability that had been seen up to that point. The magnitude of the large dynamic pressure increase triggered the procedure to command a normal corridor control maneuver that raised periapsis such that the expected dynamic pressure on the next orbit would be less than 0.3 N/m², even if the density remained at the unusually high value from the preceding orbit. At about the time the periapsis raise maneuver was taking place, the dust observation data became available. The observations of the dust levels, primarily from the thermal emission spectrometer (TES) that was onboard the MGS S/C, showed evidence of increasing dustiness. (These were later confirmed by the microwave observations made by Clancy from the Kitt Peak Radio Telescope.) Because the large density increase that had

just been detected could be the start of a continued larger increase associated with the start of a global dust storm, the flight operations manager wisely chose to increase the periapsis altitude even further with an extremely unusual second propulsive maneuver on the same orbit. During the next several days, the density increased by a factor of almost three before gradually returning to pre-dust-storm levels. Both the rate of density increase and the rate of decrease were more rapid than expected for a regional storm. Although the TES observations during the next month showed that the dust storm did not turn into the globally encircling kind that has the largest effect on the atmospheric densities, this regional storm in the southern hemisphere (centered on 30° south, 20° east) had a significant effect on the densities in the northern hemisphere near periapsis (at 35° north latitude on orbit 51). In keeping with a longstanding tradition, this period of intensively exciting activity occurred on a holiday, Thanksgiving.

Following the start of the dust storm on orbit 51, the dynamic pressure was kept at a low value until there was definite evidence that the dust storm was dissipating. The sparse observations of previous dust storms indicated that dust storms could start up, begin to dissipate, and then start back up again, and so the flight operations manager remained cautious and kept the dynamic pressure below planned levels until the dust storm was clearly dissipating. To make up for the slower rate of period reduction caused by the low dynamic pressures during the dust storm, the average dynamic pressure following the dust storm was increased from 0.20 to 0.25 N/m². By the time the dust storm dissipated, several techniques had been developed that enabled more accurate predictions of the dynamic pressure on the next orbit, which reduced the risk of a slightly higher average dynamic pressure. The most useful of these prediction tools was a correlation between the density and the longitude. Figure 4 shows a plot created by Justus, one of the creators of the MarsGRAM atmosphere model⁸ that shows the density ratio between the actual density at periapsis that was inferred from the accelerometer measurements and the density obtained from the MarsGRAM model. The wave 2 dependency on longitude is believed to be due to coupling of the strong polar vortex around the north pole during northern winter and the topography in the northern hemisphere. (Early results from phase 2 show a wave 3 dependency on longitude, while the polar vortex has moved to the south pole.)

Figure 3 shows that the actual dynamic pressure (+ symbols) was nearly zero during the SPO. The S/C remained in the SPO until the middle of September, when periapsis was lowered back into the atmosphere. Figure 3 also includes the planned dynamic pressures (Δ symbols) up to the aerobraking exit maneuver on Feb. 9, 1999 (orbit 1325). The dynamic pressures for the redesigned aerobraking phase are only about one-third to one-half as large as the 0.6 N/m² that was originally planned for the fully deployed solar panels, when aerodynamic heating was the primary constraint. Note that phase 2 actually started one week later than the plan because a

$$F = 0.75 + 0.05 \cdot \cos(\text{LonW}) - 0.20 \cdot \cos(2 \cdot \text{LonW})$$

RMS error = 23% of Mean
r-squared = 40%

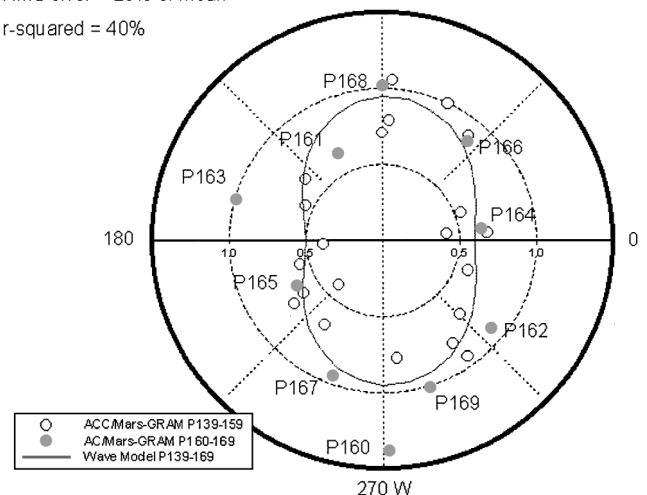


Fig. 4 Density ratio (actual/MarsGRAM) vs longitude.

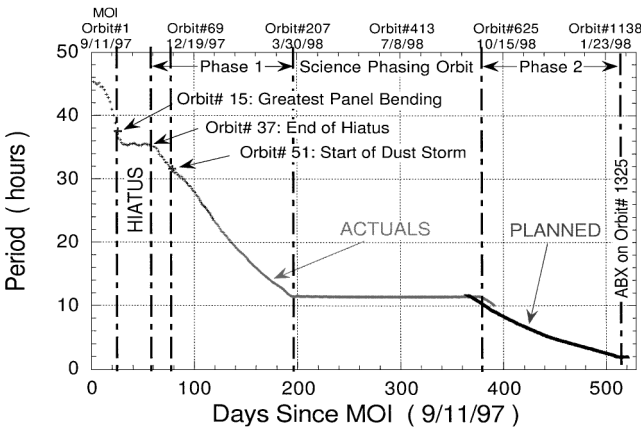


Fig. 5 Orbit periods: actual and planned.

ground software problem put the S/C into contingency mode a few minutes before the sequence was programmed to lower periapsis back into the atmosphere.

The sharp decrease in the dynamic pressure at the end of phase 2 is due to a project requirement to maintain a 2-day orbit lifetime. The lifetime is actually defined by the time required to reach an apoapsis altitude of 300 km, which is 100 km below the mapping orbit altitude. The first time the orbit reaches the 2-day orbit lifetime constraint, the apoapsis altitude will be about 916 km. The S/C would be only one or two orbits from crashing if the apoapsis ever reached the 300-km apoapsis altitude limit, and so a 300-km apoapsis is representative of the orbit lifetime. When the orbit reaches the point where a 300-km apoapsis is predicted to be only 2 days away, periapsis will be raised by a 1.1-m/s maneuver to increase the orbit lifetime back to 3 days. One day later, the orbit will have decayed to the point where the orbit lifetime is again only 2 days, and so another 1.1-m/s maneuver will be required. Trajectory simulations usually require 3 or 4 of these walkout maneuvers before apoapsis has shrunk to the point (≈ 450 km) where the aerobraking exit maneuver (ABX) can raise periapsis out of the atmosphere for the final time. The walkout phase for the original aerobraking design was much longer, 12 days rather than 3 days, in part because the dynamic pressures at the start of the walkout phase were much larger. Using a 300-km apoapsis limit to define the orbit lifetime on the last aerobraking orbit is somewhat conservative in the sense of orbit lifetime because the S/C would be able to survive for perhaps 12 more orbits beyond the 300-km apoapsis limit. Because the propellant required to get from the last survivable aerobraking orbit to the mapping orbit would be quite large, the 300-km limit has been used to indirectly limit the propellant cost in case there is a problem during the walkout phase.

The argument of periapsis drifts past the south pole before the ABX maneuver is performed in all simulated trajectories that reach the desired 2 a.m. mapping orbit. Because the desired periapsis location for the mapping orbit is at the south pole, some time will be required for periapsis to drift back to the south pole before the S/C can be propulsively locked into the sun-synchronous, nearly circular, frozen mapping orbit.

The orbit period is another key aerobraking parameter. Aerobraking will shrink the orbit period from more than 45 h at MOI to less than 2 h at ABX. Figure 5 shows the past and planned orbit periods. The rate of decrease prior to orbit 15 is much steeper than for the remainder because the original plan used a higher average dynamic pressure to finish aerobraking in only 140 days. The amount of period decrease during the hiatus was insignificant. The rate of decrease during phase 2 is expected to be slightly less than during phase 1 because the planned dynamic pressures are less. Once the orbit period has been reduced to 1.89 h, the ABX maneuver will raise periapsis out of the atmosphere.

Mapping Mission

When the MGS S/C reaches the 400-km nearly circular, sun-synchronous, 2 a.m. mapping orbit, it will begin a 2-year global mapping mission. The science instruments include the magne-

Table 2 Science instruments and investigators^a

Instrument	Principal investigator and home institution	Objective
Mag/ER	M. H. Acuna Goddard Space Flight Center	Intrinsic magnetic field and solar wind interactions with Mars
MOC	M. C. Malin Malin Space Systems	Surface and atmospheric imaging
MOLA	D. E. Smith Goddard Space Flight Center	Surface topography and gravity field studies
MR	J. Blamont Centre Nationale d'Etudes Spatiales	Relay support for future Mars Lander missions, both American and international
TES	P. R. Christensen Arizona State University	Mineralogy, condensates, dust, thermal properties, and atmospheric measurements
USO (RS)	G. L. Tyler Stanford University (team leader)	Gravity field determination and atmospheric refractivity profiles

^aDetails about the science observations may be found on the web through links from <http://mars.jpl.nasa.gov>.

tometer/electron reflectometer (Mag/ER), the Mars Orbiter camera (MOC), the thermal emission spectrometer (TES), the Mars Orbiter laser altimeter (MOLA), and an ultrastable oscillator for radio science [USO (RS)] observations. The S/C also carries a Mars relay radio system (MR) antenna for use by future missions to Mars. All of the instruments, except the relay antenna, have already made measurements of Mars. The purpose of the MGS mission is to perform a global survey of the planet Mars. The TES provides many spectral bands, which will enable scientists to characterize not only the surface mineralogy, but also the atmospheric composition and temperature. A detailed topographic map will be produced from the MOLA data, whereas the MOC will provide a visual context using both wide- and narrow-angle cameras. RS will produce a global gravity field as well as atmospheric profiles during occultations.

Investigators

The MGS mission described has been a collaboration of many teams of scientists and engineers spread all across the country. The spacecraft was built by Lockheed Martin Astronautics (LMA), and the bulk of the spacecraft operations team is located at the LMA facility near Denver, Colorado. The science instruments are operated by the principal investigators from their home facilities, which are listed in Table 2. Atmospheric monitoring and forecasting is provided by the Atmospheric Advisory Group, lead by Richard Zurek of the Jet Propulsion Laboratory (JPL). Observations are made by the onboard instruments as well as S/C telemetry measurements and ground-based microwave observations. S/C operations, including commanding, telemetry evaluation, subsystems performance analysis, and aerobraking sequencing, are performed by the S/C lead by Kenny Starnes at LMA. A special team of students lead by Gerald Keating of George Washington University measure the atmospheric density and dynamic structure using an onboard accelerometer.^{9,10} The ground-based microwave measurements from the National Radio Astronomy Observatory antenna at Kitt Peak are analyzed by Todd Clancy of the Space Science Institute. Atmospheric modeling is supplied by Jere Justus through NASA Marshall Space Flight Center, Stephen Bougher of the University of Arizona, and James Murphy and Robert Haberle of NASA Ames Research Center. Interpretation of the TES observations are provided by a team lead by John Pearl at NASA Goddard Space Flight Center. Navigation is performed by a team lead by Pasquale Esposito at the JPL. Mission design, sequencing, and ground data support are also supplied by JPL. The Mission Director, Joseph Beerer, and the Project Manager, Glenn Cunningham, are provided by JPL.

Summary

Aerobraking has enabled the MGS mission to fit within the very tight budget available for the exploration of Mars by reducing the launch vehicle cost by at least $\$1 \times 10^8$ (Ref. 11). Aerobraking has

proven to be a very robust option, enabling the mission to proceed toward what appears will be a fully successful completion, in spite of a major structural failure.

Aerobraking has also enabled new science observations at Mars that would not have been possible otherwise. Detailed measurements of the density and structure of the upper atmosphere have been made using the accelerometer that was originally used for precise propulsive maneuver cutoff. The extremely low altitudes required for aerobraking have enabled the magnetometer to observe magnetic fields at a much higher resolution than will be possible from the mapping orbit and have enabled electron reflectometer measurements above and below the ionopause, something that will be impossible from the mapping orbit. During the hiatus and the low-altitude SPO, the narrow-angle camera was able to take images at sun illumination angles that are significantly better than from the sun-synchronous mapping orbit. Targeted, high-resolution images of specific surface features were made during the SPO phase. Images, thermal spectra, and even laser altimeter measurement of Phobos were made near the end of the SPO phase.

Conclusions

Aerobraking has been a very exciting experience for everyone involved. A well thought out plan had to be significantly modified twice during flight by an operations team that was already much smaller than previous flight teams. A major structural failure and the resulting side effects of a greatly extended aerobraking phase were successfully accommodated. Dust storms and the previously suspected but unknown atmospheric dynamics had to be overcome. The MGS mission has been extremely challenging so far, and there is every reason to believe that phase 2 will be just as exciting as what has taken place so far.

Acknowledgment

Tracking and commanding are performed using the Deep Space Network.

References

¹Lyons, D. T., "Mars Global Surveyor: Aerobraking with a Broken Wing," AIAA/AAS Astrodynamics Conf., American Astronautical Society Paper

97-618, Sun Valley, ID, Aug. 1997.

²Johnston, M. D., et al., "Mars Global Surveyor: Aerobraking at Mars," AAS/AIAA Space Flight Mechanics Meeting, American Astronautical Society Paper 98-112, Monterey, CA, Feb. 1998.

³Wilmoth, R. G., Rault, D. F., Cheatwood, F. M., Englund, W. C., and Shane, R. W., "Rarefied Aerothermodynamic Predictions for Mars Global Surveyor," *Journal of Spacecraft and Rockets*, Vol. 36, No. 3, 1999, pp. 314-322.

⁴Lee, W., and Sidney, W., "Mission Plan for Mars Global Surveyor," AAS/AIAA Flight Mechanics Conf., American Astronautical Society Paper 96-153, Austin, TX, Feb. 1996.

⁵Beerer, J., Brooks, R., Esposito, P., Lyons, D., Sidney, W., Curtis, H., and Willcockson, W., "Aerobraking at Mars: the MGS Mission," AIAA Paper 96-0334, Jan. 1996.

⁶Dallas, S., "The Mars Global Surveyor Mission," *1997 IEEE Aerospace Conference Proceedings*, Inst. of Electrical and Electronics Engineers, New York, 1997, pp. 173-179.

⁷Esposito, P. B., Johnston, M. D., Alwar, V., Demcak, S. W., Graat, E. J., and Mase, R. A., "Mars Global Surveyor Navigation and Aerobraking at Mars," 13th International Conf. on Space Flight Dynamics, American Astronautical Society Paper 98-384, Greenbelt, MD, May 1998.

⁸Justus, C. G., and James, B. J., "Recent and Planned Improvements in the Mars Global Reference Atmosphere Model (MarsGRAM)," *Advances in Space Research*, Vol. 19, No. 8, 1997, pp. 1223-1231.

⁹Keating, G. M., Bougher, S. W., Zurek, R. W., Tolson, R. H., Cancro, G. J., Noll, S. N., Parker, J. S., Schellenburg, T. J., Shane, R. W., Wilkerson, B. L., Murphy, J. R., Hollingsworth, J. L., Haberle, R. M., Joshi, M., Pearl, J. C., Conrath, B. J., Smith, M. D., Clancy, R. T., Blanchard, R. C., Wilmoth, R. G., Rault, D. F., Martin, T. Z., Lyons, D. T., Esposito, P. B., Johnston, M. D., Whetzel, C. W., Justus, C. G., and Babicke, J. M., "The Structure of the Upper Atmosphere of Mars: First in Situ Measurements from an Orbiting Spacecraft," *Science*, Vol. 279, March 13, 1998, pp. 1672-1676.

¹⁰Tolson, R. H., Keating, G. M., Cancro, G. J., Parker, J. S., Noll, S. N., and Wilkerson, B. L., "Application of Accelerometer Data to Mars Global Surveyor Aerobraking Operations," *Journal of Spacecraft and Rockets*, Vol. 36, No. 3, 1999, pp. 323-329.

¹¹Lyons, D. T., "Aerobraking: The Key to Affordable Mars Exploration," 2nd International Low-Cost Spacecraft Conf., International Academy of Astronautics, IAA Paper L-0512, Laurel, MD, April 1996.

R. D. Braun
Guest Editor